SURFACE ROUGHNESS WAKEFIELD IN FEL UNDULATOR*

G. Stupakov
SLAC National Accelerator Laboratory, Menlo Park, CA, USA
S. Reiche
Paul Scherrer Institute, Villigen-PSI, Switzerland

Abstract

We derive wakefield of a round pipe with a sinusoidal wall modulation and use this model for study of wakefields due to wall roughness of the undulator vacuum chamber of free electron lasers.

INTRODUCTION

In free electron lasers the wakefield due to the wall roughness of the vacuum chamber in the undulator can have important implications on the required smoothness of the beam tube. Detailed theoretical studies of the roughness induced impedance has been carried out in the past [1–4] and provided a useful tool for computation of the wakes and practical recommendations for the undulator vacuum chamber design.

Among several wakefield models a simple sinusoidal wall modulation with a small ratio of height to wavelength is especially attractive because of its simplicity [5]. The model neglects a so called resonant mode wakefield [6, 7] because, as it was shown in [8], the contribution of the resonant mode is small for a shallow wall perturbation. The wake derived in [5] has a singularity at the origin and shows a typical resistive behavior. While the wake singularity is integrable, and applied to a smooth beam profile gives a finite wakefield, it requires a special care in implementation of the numerical algorithm. In addition, for some idealized beam profiles, such as flat-top, the resulting bunch wake exhibits non-physical singularities at the beam edges.

In this paper we generalize the result of [5] to include the effect of the resonant mode. As it turns out this also eliminates the wake singularity at the origin and facilitates numerical calculations of wakes.

SINUSOIDAL WALL MODULATION

We consider a round pipe of radius a and represent the roughness profile of the wall by a sinusoidal perturbation

$$r = a - h \sin \kappa z, \tag{1}$$

where $2\pi/\kappa$ is the period of corrugation, and h is its amplitude. It is assumed that both the wavelength and the amplitude are small compared to the pipe radius, $h \ll a$ and $\kappa a \ll 1$. This allows one to neglect in calculations the curvature of the round wall and to consider the surface locally as a plane one. It is also assumed that the corrugation is shallow,

$$h\kappa \ll 1, \tag{2}$$

that is the amplitude of the corrugation bumps is much smaller then their period.

Using the perturbation theory developed in [1], the following expression for the wakefield (per unit length of pipe) of a point charge was obtained in [5]

$$w(s) = \frac{h^2\kappa^3}{a} f(\kappa s), \tag{3}$$

where the function f is

$$f(\zeta) = \frac{1}{2\sqrt{\pi}} \frac{\partial}{\partial \zeta} \frac{\cos(\zeta/2) + \sin(\zeta/2)}{\sqrt{\zeta}}, \tag{4}$$

for $\zeta > 0$ and $f = 0$ otherwise. The wake function in (3) is defined so that positive w corresponds to the energy loss, and positive s corresponds to the test particle behind the source one. The plot of this function is shown in Fig. 1. One can see that $f(\zeta)$ has a singularity at the

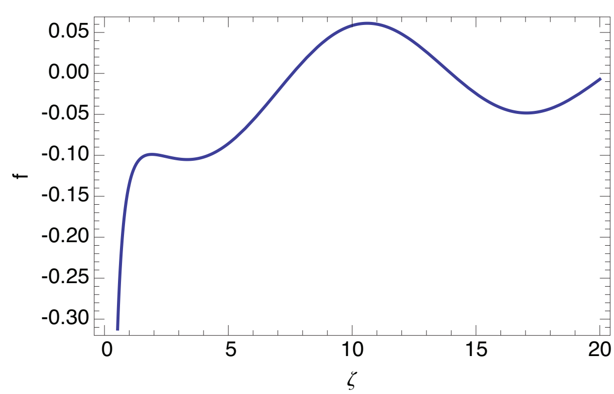

Figure 1: Function $f(\zeta)$.

origin, $f \propto \zeta^{-3/2}$, similar to the resistive wall wake in a round pipe in the standard approximation [9] of long wavelengths. The negative sign of the wake (3) near the origin seems to suggest that the source charge gains energy in the process of interaction with the wall. This conclusion however is incorrect as we will see below.

In a seemingly different approach to the problem, using the concept of surface impedance of the sinusoidal corrugation (1), an expression for the beam longitudinal impedance

* Work supported by the U.S. Department of Energy under contracts No. DE-AC02-76SF00515.

ISBN 978-3-95450-126-7

was derived in [8],

$$Z(k) = \frac{2\zeta(k)}{ac} \frac{1}{1 + ka\zeta(k)/2i}, \tag{5}$$

where $k = \omega/c$ and

$$\zeta(k) = \frac{1}{4} k h^2 \kappa^{3/2} \frac{\sqrt{2k+\kappa} - i\sqrt{2k-\kappa}}{\sqrt{4k^2-\kappa^2}}. \tag{6}$$

In case $2k < \kappa$ the square roots of the negative values in this expression should be taken with a positive imaginary part. The impedance (5) is defined for positive k; for $k < 0$ one should use $Z(-k) = Z^*(k)$. It was shown in [8] that in the limit of long wavelengths, $k \ll \kappa$, the impedance (5) supports a resonant mode previously found in [6, 7].

A natural question arises: how does the wake (3) relates to the impedance (5)? As it turns out, the wake (3) can be obtained from (5) if one neglects the term with ζ in the denominator of (5), that is using

$$Z(k) = \frac{2\zeta(k)}{ac}. \tag{7}$$

This can be easily established by substituting the wake (3) into the relation between the longitudinal wake and impedance

$$Z(k) = \frac{1}{c} \int_{-\infty}^{\infty} w(s) e^{iks} ds, \tag{8}$$

integrating (8) by parts, and using the integral $\int_0^\infty e^{iqs} s^{-1/2} ds = (i\pi/q)^{1/2}$.

AN IMPROVED WAKEFIELD MODEL

It is now clear that if one uses (5) rather than (7) for the impedance, one obtains a more general than (3) expression for the wake. As was mentioned above the impedance (5) supports the resonant mode, hence the new wake will also accommodate this feature. Substituting (5) into $w(s) = (c/2\pi)\int_{-\infty}^{\infty} Z(k) e^{-iks} dk$ we obtain

$$w(s) = \frac{1}{\pi a} \int_{-\infty}^{\infty} \frac{\zeta(k) e^{-iks} dk}{1 + ka\zeta(k)/2i} = \frac{4}{a^2} H(\kappa s, r), \tag{9}$$

where

$$\begin{aligned} H(\tau, r) &= \frac{r}{2\pi} \int_{-\infty}^{\infty} \frac{S(q) e^{-iq\tau} dq}{1 - irqS(q)} \\ &= \frac{r}{\pi} \mathrm{Re} \int_0^\infty \frac{S(q) e^{-iq\tau} dq}{1 - irqS(q)}, \end{aligned} \tag{10}$$

with

$$S(q) = q \frac{\sqrt{2q+1} - i\sqrt{2q-1}}{\sqrt{4q^2-1}}, \tag{11}$$

and

$$r = \frac{1}{8} h^2 \kappa^3 a. \tag{12}$$

Note that in the region $0 < q < \frac{1}{2}$ the function $S(q)$ is purely imaginary, with the negative imaginary part that takes values from 0 to $-\infty$. This means that the integrand in (10) has a pole in this region whose position q_* is determined from the equation

$$q_* \mathrm{Im}\, S(q_*) = -\frac{1}{r}.$$

The integration path in (10) should bypath this pole in the upper half-plane of the complex variable q as shown in Fig. 2 by red line. The contribution of this pole to the wake

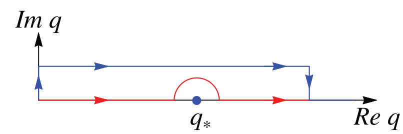

Figure 2: Integration contour (red) in the complex plane of variable q. The blue line shows another possible integration path.

w gives an oscillating with distance term $\propto e^{-iq_*\kappa s}$ which is interpreted as a contribution of the resonant mode with the wavenumber κq_*. In the limit $r \to 0$, that is the limit of extremely small amplitudes of the corrugation, $q_* \to \frac{1}{2}$ and the synchronous mode has a wavelength equal to twice the wavelength of the corrugation. In practice, a more convenient for integration path can be chosen, as shown by the blue line in Fig. 2; such a path was used in this work for calculation of wakes presented in the subsequent sections.

Asymptotically, for $q \to \infty$, the function S increases as $S \propto \sqrt{q}$ which results in a rather poor convergence of the integral (10) at infinity. The convergence can be accelerated by noting that for positive τ and r, $\mathrm{Re} \int_0^\infty e^{-iq\tau} dq (1 + irq)^{-1} = 0$, and adding this integral to (10):

$$H(\tau, r) = \frac{r}{\pi} \mathrm{Re} \int_0^\infty e^{-iq\tau} dq \frac{S(q) + 1}{[1 - irqS(q)](1 + irq)}. \tag{13}$$

The integrand in (13) decays at $q \to \infty$ much faster, as $\propto 1/q^2$, which improves the convergence of the integral and facilitates numerical calculation of the wake.

Note that the wakefunction defined by (9) and (13) is finite (and positive) at $s = 0$. The positive wake corresponds to the energy loss of the charge due to the wake, and resolves the issued raised in the previous section in connection with the negative singularity of function $f(\zeta)$. Also note that $H(0, r) = 1$ which means that the wake at the origin is $w(s = 0) = 4/a^2$. As discussed in Ref. [10], this value, arising in many problems in round geometry, is universal for the wake at the origin.

In some cases, for numerical calculations of the wake it is convenient to deal with the integrated wake

$$g(s) = \int_0^s w(s') ds' = \frac{4}{\kappa a^2} G(\kappa s, r), \tag{14}$$

ISBN 978-3-95450-126-7

where

$$G(\tau, r) = \int_0^{\tau} H(\tau', r) d\tau'. \quad (15)$$

Function G can be computed directly from the Fourier representation (13)

$$G(\tau, r) = \frac{r}{\pi} \mathrm{Im} \int_0^{\infty} dq \frac{(1 - e^{-iq\tau})(S(q) + 1)}{q[1 - irqS(q)](1 + irq)}. \quad (16)$$

Again, the integration here bypasses the pole at $q = q_*$ as shown in Fig. 2.

EXAMPLE OF SWISSFEL WAKE

We consider here two practical examples relevant for the SwissFEL project at PSI [11]. For the roughness parameters we assume $h = 100$ nm, $2\pi/\kappa = 10$ micron with the pipe radius $a = 2$ mm. Substituting these numbers into (12) gives $r = 0.62$. The plot of the point charge wake for this case computed with the help of Eqs. (9) and (13) is shown in Fig. 3 by blue line. For comparison, the red line

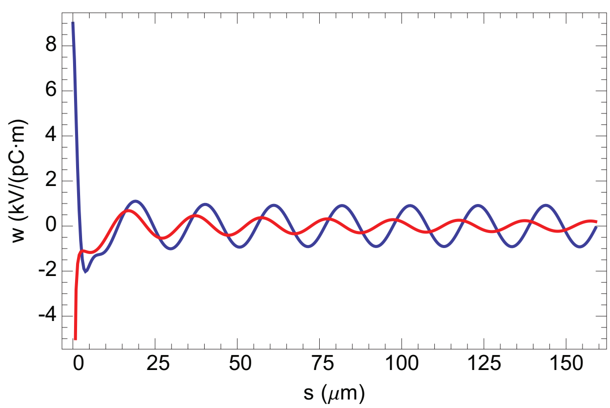

Figure 3: Wake for a point charge for parameters listed in the text.

shows the singular wake given by (3) and (4). Note that the new wake is positive near the origin, as discussed in the previous section. Also noticeable are more pronounced oscillations of the new wake which are due to the resonant mode.

The wake for a Gaussian bunch with $Q = 200$ pC and the rms bunch length of 8 microns (corresponding to the peak current of 3 kA) is shown in Fig. 4 by the blue line. The red line shows the bunch wake calculated with the singular Green function (3). The difference in this case between the two models is not large.

In the low-charge operational mode the bunch charge is 10 pC and the rms bunch length is 0.8 microns (corresponding to the peak current of 1.5 kA). The wake calculated in this case is shown in Fig. 5 with the blue and red lines corresponding to the new and old wake models, respectively. Notice a considerable difference between the models. It

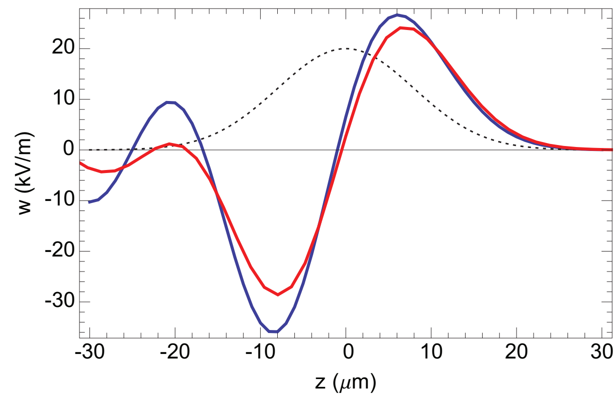

Figure 4: Wake of a Gaussian bunch with $Q = 200$ pC. The red line is computed with the singular Green function (3) and the blue line is computed with the new Green function (9). The dashed line shows the Gaussian bunch profile with the bunch head on the right.

turns out that such a short bunch excites the resonant mode (the mode is clearly visible behind the bunch, in the region not shown in Fig. 5).

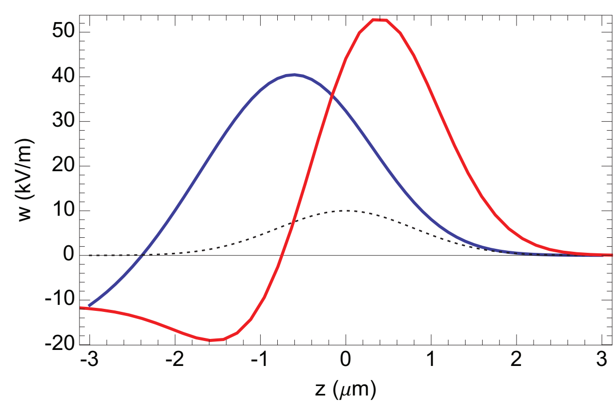

Figure 5: Wake of a Gaussian bunch with $Q = 10$ pC. The red line is computed with the singular Green function (5) and the blue line is computed with the new Green function (9). The dashed line shows the Gaussian bunch profile with the bunch head on the right.

EXAMPLE OF NGLS WAKE

In another example we calculated the roughness wakefield for the soft x-ray FEL project being developed at Berkeley National Accelerator Laboratory [12]. Three different amplitudes of the corrugation were considered: $h = 100$ nm, $h = 200$ nm and $h = 500$ nm. In this case we assumed that the rms roughness angle is 10 mrad, corresponding to the product $\varkappa h = \sqrt{2} \cdot 10^{-2}$. Respectively, for

ISBN 978-3-95450-126-7

each amplitude we found the wavelength of the corrugation $\lambda = 2\pi/\kappa$: $\lambda = 44\ \mu$m, $\lambda = 88\ \mu$m and $\lambda = 220\ \mu$m.

For the electron beam profile in the NGLS undulator we used the result of a start-to-end computer simulation [13] shown in Fig. 7. The simulated beam profile was smoothed

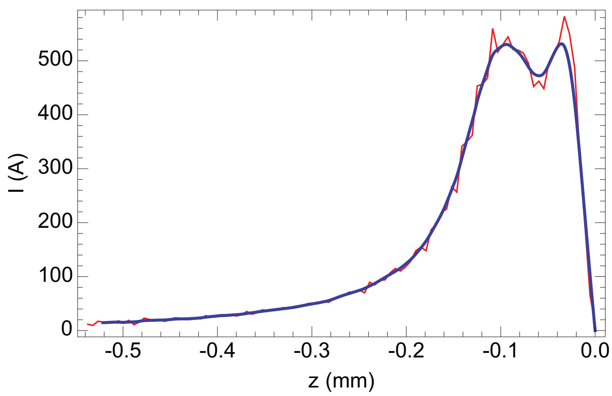

Figure 6: Beam profile at NGLS used for calculation of the wake. The red curve shows the original simulation, and the blue curve is a smoothed profile used for calculation of the wakes. The head of the bunch is on the right.

out as shown in Fig. 6 for the wake calculations.

The wakefield for the parameters indicated at the beginning of this section are shown in Figs. 7-9.

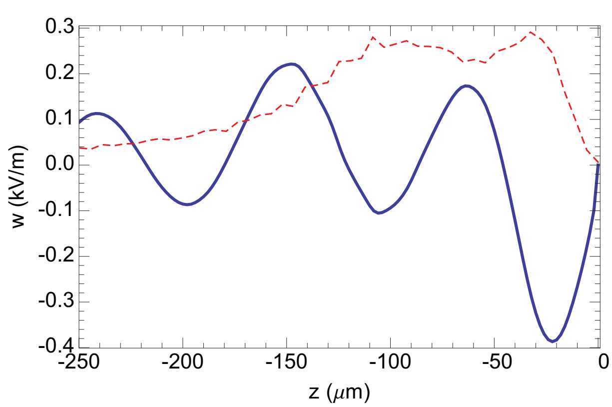

Figure 7: Wakefield for $h = 100$ nm. The red dashed curve shows the beam profile.

The amplitude of the wake somewhat increases with the amplitude of sinusoidal wall modulation, however, the effect is not strongly pronounced due to the simultaneous increase of the roughness wavelength.

CONCLUSIONS

In this paper we derived a new improved model for the roughness wake in the model where roughness is approximated by a sinusoidal wall modulation with a given amplitude and wavelength. The new wake is finite at the origin

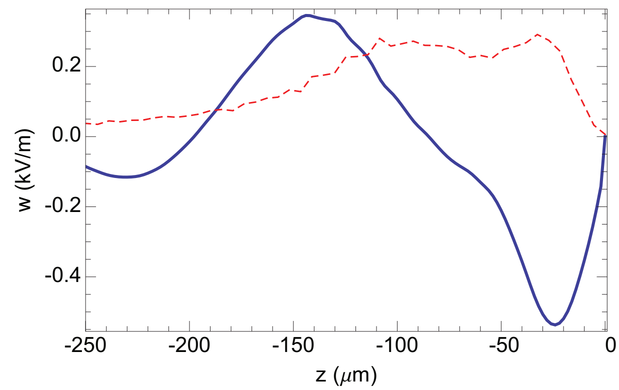

Figure 8: Wakefield for $h = 200$ nm. The red dashed curve shows the beam profile.

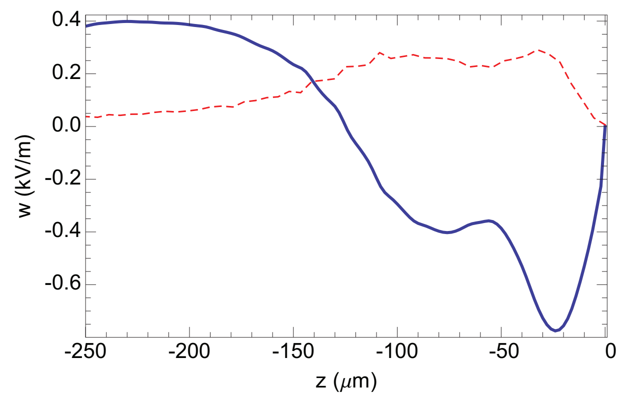

Figure 9: Wakefield for $h = 500$ nm. The red dashed curve shows the beam profile.

and incorporates a so called resonant mode. An analytical expression for the wake Green function is derived and applied to calculation of several examples for the SwissFEL and NGLS projects.

REFERENCES

[1] G. V. Stupakov, Phys. Rev. ST Accel. Beams **1**(6), 064401 (1998).

[2] K. L. F. Bane and G. V. Stupakov, in *International Computational Accelerator Physics Conference (ICAP 98)*, Monterey, CA (1998).

[3] G. V. Stupakov, in S. Chattopadhyay, M. Cornacchia, I. Lindau, and C. Pelegrini, eds., *Arcidosso 2000, Physics of, and science with, the X-ray free-electron laser*, Arcidosso, Italy (September 10 – 15 2000), no. 581 in AIP Conference Proceedings, pp. 382–386.

[4] K. Bane and G. Stupakov, in *20th International Linac Conference (Linac 2000)*, Monterey, California (2000), vol. 1, pp. 92–94.

[5] G. Stupakov, in S. Chattopadhyay, M. Cornacchia, and C. Pelegrini, eds., *Nonlinear and Collective Phenomena in Beam Physics 1998 Workshop*, New York (1999), no. 468 in AIP Conference Proceedings, pp. 334–47.

ISBN 978-3-95450-126-7

[6] A. Novokhatski and A. Mosnier, in *Proceedings of the 1997 Particle Accelerator Conference* (IEEE, Piscataway, NJ, 1997), pp. 1661–1663.

[7] K. L. F. Bane and A. Novokhatskii, *The Resonator impedance model of surface roughness applied to the LCLS parameters*, Tech. Rep. SLAC-AP-117, SLAC (March 1999).

[8] G. V. Stupakov, in T. Roser and S. Y. Zhang, eds., *Workshop on Instabilities of High Intensity Hadron Beams in Rings* (American Institute of Physics, Upton, New York, 1999), no. 496 in AIP Conference Proceedings, pp. 341–350.

[9] A. W. Chao, *Physics of Collective Beam Instabilities in High Energy Accelerators* (Wiley, New York, 1993).

[10] K. L. F. Bane and G. V. Stupakov, Phys. Rev. ST Accel. Beams **6**, 024401 (2003).

[11] *SwissFEL Conceptual Design Report*, Tech. Rep. 10-04 (2012).

[12] J. Corlett, A. Allezy, D. Arbelaez, J. Byrd, C. Daniels, S. D. Santis, W. Delp, P. Denes, R. J. Donahue, L. Doolittle, *et al.*, in *Proceedings of the 2013 FEL Conference*, New York, USA (2013).

[13] P. Emma, private communication.

ISBN 978-3-95450-126-7